西安交通大学
XI'AN JIAOTONG UNIVERSITY

World Scientific
www.worldscientific.com

Impedance spectra of different capacitor technologies

René Kalbitz

Würth Elektronik eiSos GmbH, Headquarters
Max-Eyth-Straße 1, Waldenburg 74638, Germany

Product Unit Capacitors & Resistors, Competence Center Berlin
Volmerstraße 10, Berlin 12489, Germany
Rene.Kalbitz@we-online.de

This paper reviews the interpretation of impedance and capacitance spectra for different capacitor technologies and discusses how basic electrical characteristics can be inferred from them. The basis of the interpretation is the equivalent circuit for capacitors. It is demonstrated how the model parameters, such as capacitance and equivalent series resistance, can be extracted from the measured spectra. The aspects of measurement accuracy are exemplarily discussed on the measured spectra.

Keywords: Impedance; capacitance; spectra; capacitors; equivalent circuit; equivalent series resistance; measurement accuracy.

1. Introduction and Theoretical Background

Impedance and capacitance spectra (or scattering parameters) are common representations of frequency- dependent electrical properties of capacitors. The interpretation of such spectra provides a wide range of electrochemical, physical and technically relevant information. Those need to be separated from the ever-present measurement artifacts as well as parasitic effects.

Since it is sometimes not possible to provide all data in the datasheet, the electrical engineer may have to utilize the measured spectra to choose the suitable component for the circuit design. Würth Elektronik eiSos implemented the public online tool Redexpert, where spectra and other measurements are provided.

This paper recapitulates the properties of such spectra and discusses how basic electrical characteristics can be inferred from them.

1.1. Equivalent circuit of capacitors

With the circuit, shown in Fig. 1, it is possible to model frequency-dependent impedance spectra of all capacitor types ranging from multilayer ceramic capacitors (MLCC) to Supercapacitors (SCs).[1–4]

The formula symbol C_S is pure capacitance, which does not exist on its own as an electrical component. Any real capacitor has losses, which "slows down" the charge storing process. This phenomenon is modeled by the pure Ohmic equivalent series resistance R_{ESR} (ESR). The resistance of the current collector electrodes and the leads also contribute to the ESR.

The pure lossless capacitance is defined by a differential equation:

$$C_S = \frac{dQ}{dV}, \tag{1}$$

with dQ as the change of charge at the capacitor interface and dV as the change of voltage at the capacitor.

Any alternating current in a metal conductor induces a magnetic field that opposes the current. In our model, this property is described by the equivalent series inductance L_{ESL} (ESL). Sometimes it is also referred to as parasitic inductance. C_S, R_{ESR} as well as L_{ESL} are the most important parameters, necessary to describe the majority of all spectra. In the most basic approach, they are constants and do not change with frequency, which is sufficiently accurate for electrical engineering.

The loss of charges over time, i.e., the leakage current, is described in good approximation by the pure Ohmic resistance R_{Leak}. Usually, R_{Leak} is magnitudes larger than R_{ESR} and can often be neglected, i.e., $R_{Leak} \to \infty$. As we will see, its effect may only be visible in the spectra at very low frequencies below 1 Hz or so. A correct description of leakage current is, however, a physically complex issue, which may depend on further parameters such as pre-polarization time and temperature. For technical measurement reasons, it is therefore a common practice not to state R_{Leak} but the value of leakage current, along with its measurement conditions in the datasheet.

This equivalent circuit in Fig. 1 also yields the possibility to model practically any
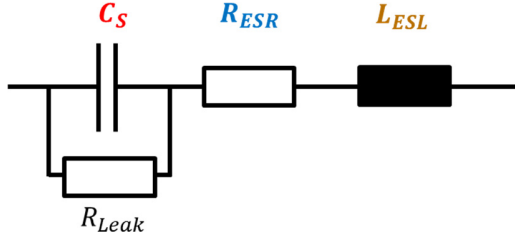
• voltage,

Fig. 1. Standard equivalent circuit as used for capacitors.

- environmental (e.g., temperature) or
- nonlinear frequency

dependency. In this case, all model parameters are simply replaced by suitable mathematical functions, or entire circuit sections are replaced by distributed networks.[3,5–8]

2. The Impedance and Capacitance Spectra

In the following paragraph, we define frequently used terms and measured quantities, such as capacitance and impedance.[1]

The above circuit can be expressed as frequency-dependent complex impedance $\hat{Z}$, capacitance $\hat{C}$, scattering parameter (S-Paramter) $\hat{S}$, permittivity $\hat{\epsilon}$ or any other measurable complex electrical quantity. Passive components are often characterized in terms of capacitance and impedance. We will therefore lay the focus on these two quantities.

Impedance $\hat{Z} = \mathrm{Re}(\hat{Z}) + i \cdot \mathrm{Im}(\hat{Z})$, is a complex quantity, with $\mathrm{Re}(\hat{Z})$ and $\mathrm{Im}(\hat{Z})$ as real and imaginary part, respectively. Symbol i denotes the imaginary unit, defined as $i^2 = -1$. It is often expressed in terms of its magnitude $|\hat{Z}|$ and phase angle ϕ,[2]

$$\hat{Z} = |\hat{Z}| \cdot e^{i\phi}. \qquad (2)$$

In a complex plane, as given in Fig. 2, ϕ describes the angle between $\mathrm{Re}(\hat{Z})$ (abscissa) and the complex vector $\hat{Z}$. Physically, $|\hat{Z}|$ represents the ratio of the voltage amplitude to
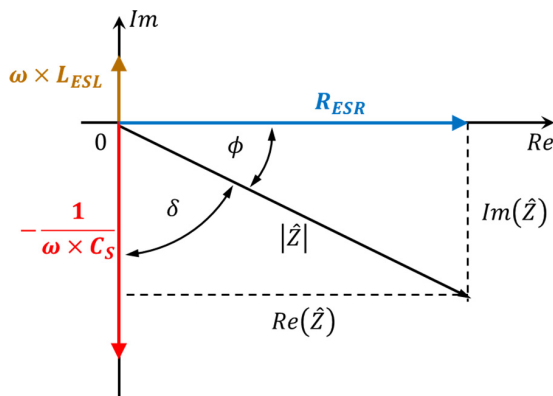

Fig. 2. Vector representation of impedance in the complex plane. R_{Leak} is neglected for the sake of simplicity.

the current amplitude, while ϕ gives the phase difference between voltage and current at a given frequency. The phase angle ϕ is related to the loss angle with

$$\arctan\left(\frac{\mathrm{Re}(\hat{Z})}{|\mathrm{Im}(\hat{Z})|}\right) = \delta = \frac{\pi}{2} - \phi, \qquad (3)$$

In electrical engineering, it is also common to use magnitude $|\hat{Z}|$ and its equivalent series resistance $R_{\mathrm{ESR}} = \mathrm{Re}(\hat{Z})$. With the model in Fig. 1, the equivalent series resistance is the real part of the impedance. To graphically show the relation between the model and complex quantity $\hat{Z}$, all model parameters (apart from R_{Leak}) are also given in Fig. 2. (Mathematical description is given in the Appendix.)

The impedance may also be transferred into complex capacitance with

$$\hat{C} = \frac{1}{i \cdot 2 \cdot \pi \cdot f \cdot \hat{Z}} = \mathrm{Re}(\hat{C}) + i \cdot \mathrm{Im}(\hat{C}). \qquad (4)$$

All these quantities, such as $\mathrm{Re}(\hat{Z})$, $\mathrm{Im}(\hat{Z})$, $|\hat{Z}|$ or δ, can be measured with impedance or network analyzers. Any electronic part (not only capacitors) can be characterized by a pair of frequency-dependent quantities, such as $\mathrm{Re}(\hat{Z})$ and $\mathrm{Im}(\hat{Z})$ or $\mathrm{Re}(\hat{C})$ and $\mathrm{Im}(\hat{C})$. However, it is only due to equivalent circuits such as those given in Fig. 1, by that measurement results can be interpreted. The model (also referred to as the standard model) provides the mathematical means to extract the electric parameters C_S, R_{ESR}, L_{ESL} and R_{Leak}.

It is not only possible to use the model for the extraction of parameters but it can also be used to calculate the theoretical spectra.

By changing C_S, R_{ESR}, L_{ESL}, R_{Leak}, it is possible to describe or calculate the basic frequency behavior for all capacitors. This is exemplarily demonstrated by impedance and capacitance spectra of a $4.7\,\mu\mathrm{F}$ and a $50\,\mathrm{F}$ capacitor, given in Figs. 3 and 4, respectively. The associated phase and loss angles are shown in Figs. A.3–A.6 in the Appendix. The parameters for the two examples are as follows:

- Supercapacitor (WCAP-STSC) with $C_S = 50\,\mathrm{F}$, $R_{\mathrm{ESR}} = 15\,\mathrm{m\Omega}$, $L_{\mathrm{ESL}} = 5\,\mathrm{nH}$ and $R_{\mathrm{Leak}} = 10\,\mathrm{M\Omega}$,
- Film capacitor (WCAP-FTBE) with $C_S = 4.7\,\mu\mathrm{F}$, $R_{\mathrm{ESR}} = 5\,\mathrm{m\Omega}$, $L_{\mathrm{ESL}} = 5\,\mathrm{nH}$ and $R_{\mathrm{Leak}} = 10\,\mathrm{M\Omega}$.

The parameters were chosen such as to fit actual Würth Elektronik eiSos products found under the match code for film capacitors WCAP-FTBE ($4.7\,\mu\mathrm{F}$) and SCs WCAP-STSC ($50\,\mathrm{F}$). In these plots, C_S, R_{ESR}, L_{ESL} and R_{Leak} were assumed to be constants and independent of frequency (Table 1). This assumption is in most cases in good agreement with actual measurements. However, especially for the R_{ESR} a frequency dependence in real measurements is noticeable, as will be discussed in the following sections.

As mentioned above, we may also think of it the other way around. With this single model, it is possible to derive the product parameters from a measured curve.
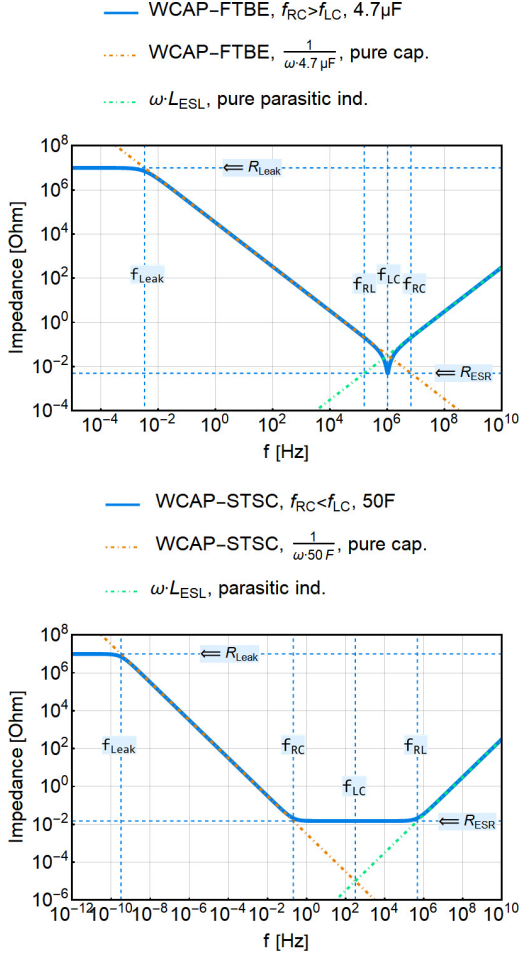
Table 1. Electrical parameters used for calculation of spectra.

Electrical prop.	WCAP-FTBE	WCAP-STSC
C_S	$4.7\,\mu\text{F}$	$50\,\text{F}$
$R_{\text{ESR}}\,[\text{m}\Omega]$	5	15
$L_{\text{ESL}}\,[\text{nH}]$	5	5
$R_{\text{Leak}}\,[\text{M}\Omega]$	10	10

Before we look at the measured graphs, it is worth the while to have a look at the theoretical graphs. They have the advantage that they can be generated for any frequency range, which allows the representation of all features, such as characteristic frequencies, in one graph.[3]

Generally, the positions of the most prominent features of the spectra are described by four characteristic frequencies:

- Characteristic frequency of the $R_{\text{ESR}} - C$ unit:

$$f_{\text{RC}} = \frac{1}{2 \cdot \pi \cdot R_{\text{ESR}} \cdot C_S} \tag{5}$$

- Characteristic frequency of the $L - C$ unit:

$$f_{\text{LC}} = \frac{1}{2 \cdot \pi \cdot \sqrt{L_{\text{ESL}} \cdot C_S}} \tag{6}$$

- Characteristic frequency of the $R_{\text{Leak}} - C$ unit:

$$f_{\text{Leak}} = \frac{1}{2 \cdot \pi \cdot R_{\text{Leak}} \cdot C_S} \tag{7}$$

- Characteristic frequency of the $R_{\text{ESR}} - L$ unit:

$$f_{\text{RL}} = \frac{R_{\text{ESR}}}{2 \cdot \pi \cdot L_{\text{ESL}}}. \tag{8}$$

Two main situations can be distinguished in Figs. 3 and 4:

- Lorentz-Oscillation: $f_{\text{RC}} > f_{\text{LC}}$ as in the case for $C_S = 4.7\,\mu\text{F}$ (blue graph) and
- Debye-Relaxation: $f_{\text{RC}} < f_{\text{LC}}$ as in the case for $C_S = 50\,\text{F}$ (orange graph).[9,10]

f_{RC}, the characteristic frequency of the RC unit, is the frequency at which the capacitor can be charged and discharged. The inverse of the frequency is basically the charging time under ideal constant voltage charging. For the capacitor with $C_S = 50\,\text{F}$, the ideal charging time is about $2 \cdot \pi \cdot 15\,\text{m}\Omega \cdot 50\text{F} \approx 5\,\text{s}$. Below the frequency of $(5\,\text{s}^{-1})$ the capacitor can utilize its nearly full capacitance ($> 99.3\%$). Above this frequency, the capacitor is not fully charged anymore (in reference to the maximum voltage of the AC signal).

At f_{RC} the capacitance spectrum (Fig. 4) of the super-capacitor shows a shoulder. Below this frequency, the capacitance value can be inferred from the graph. Above f_{RC} the impedance spectrum, given in Fig. 3 (Bottom), shows a plateau at R_{ESR}.

Fig. 3. (Color online) Impedance spectra $|\hat{Z}|$ for WCAP-FTBE (Top) and WCAP-STSC (Bottom) as calculated from the standard model. The dashed-dotted orange and green lines in both graphs signify the pure capacitive and inductive parts.
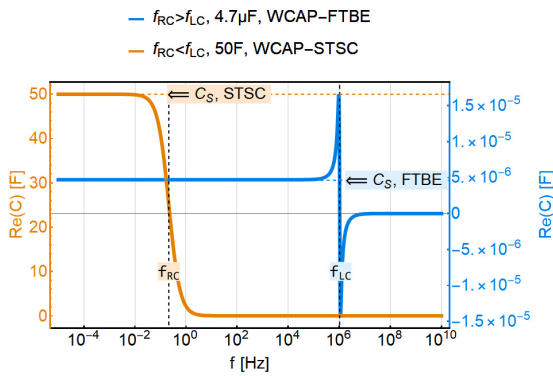
Fig. 4. (Color online) Capacitance spectra $\text{Re}(\hat{C})$ as calculated from the standard model. The graph for WCAP-STSC (orange) corresponds to the left-hand ordinate and the graph for the WCAP-FTBE (blue) corresponds to the right-hand ordinate. For the imaginary part of the capacitance, please refer Fig. A.1 in the Appendix. The horizontal dashed lines designate the pure capacitive contributions.

f_{LC}, the characteristic frequency of the L-C unit, is the frequency at which the coupling of parasitic inductance and capacitance leads to a resonant behavior (if $f_{RC} > f_{LC}$). Below this frequency, the capacitor acts as a capacitor, i.e., can be charged. Above this frequency, the capacitor acts as an inductor. The self-resonance results in a sharp minimum in the impedance spectrum (WCAP-FTBE), as given in Fig. 3 (Top). At the minimum of the impedance spectrum, the R_{ESR} value can be read off. Capacitors should not be operated at f_{LC} or above this frequency.

The capacitance spectrum (WCAP-FTBE) in Fig. 4 shows a pole, which is a special type of singularity. It is actually a real physical behavior and not only a measurement artifact.

The measurement system, which consists of the capacitor and the parasitic inductance, behaves like an oscillator, i.e., resonator.[9]

At the increasing positive branch, the probing signal constructively contributes to the oscillations of the resonator. That is to say, the charge increase dQ at the interface is disproportionately high, although the magnitude of applied voltage signal dV remains the same. Since $C_S = \frac{dQ}{dV}$, a strong increase of the capacitance is measured. At the maximum, the system is in phase (resonance) with the probing signal.

A further increase of the probing frequency leads to an abrupt change in sign of the capacitance (singularity) at f_{LC}.

At the negative branch, the probing signal destructively overlaps with the oscillations of the resonator. The current is actually flowing "in opposite direction" to the probing voltage.

Thus, the applied voltage signal dV leads effectively to a relative decrease of charge at the capacitor interface $-dQ$, which results in a negative capacitance.

f_{Leak} is the characteristic frequency of the $R_{Leak} - C$ unit. Below this frequency, the capacitor acts like a resistor with resistance R_{Leak}. That is to say, at very low frequencies, the leakage discharge is larger than the AC charging current. Usually, this effect is barely visible in the spectra. It requires either measurements to frequencies below 1 Hz or a rather low R_{Leak}.

f_{RL}, the characteristic frequency of the $R_{ESR} - L$ unit, is the frequency above which the capacitor acts like an inductor with inductance L_{ESL} (Fig. 3, bottom). In cases where $f_{RC} < f_{LC}$, it signifies the onset of the increase in impedance at high frequencies. Above this frequency, it is exceedingly difficult to extract R_{ESR} values from the measured impedance spectra.

2.1. *Measured impedance spectra and capacitance spectra*

The following sections will discuss spectra on different capacitor types, exemplarily chosen from the Würth Elektronik eiSos portfolio. The standard model, depicted in Fig. 1, uses a frequency-independent Ohmic resistance R_{ESR}. However, physical processes as well as measurement artifacts may lead to deviations from the idealized Ohmic behavior, as will be seen in the following section.[8,11]

2.2. *Supercapacitors, WCAP-STSC*

The spectra presented below were measured with the impedance analyzer Alpha-AK, POT/GAL from Novocontrol in a four-terminal Kelvin configuration. The four-terminal Kelvin configuration has the advantage of enabling a high phase angle resolution of about $0.001°$, since the voltage measurement probes are independent of the current supply leads.

The measured impedance spectrum of a SC with 50 F in Fig. 5 shows the same features as the corresponding theoretical spectrum in Fig. 3.

In this case ($f_{RC} < f_{LC}$), f_{RC} is below 1 Hz and is thus several orders of magnitudes smaller than f_{LC}. As a result, the spectrum shows a flat bottom region from which R_{ESR} can be inferred. The increase of R_{ESR} towards lower frequencies is more clearly visible in the spectrum of $\text{Re}(\hat{Z}) = R_{ESR}$ in Fig. 6.
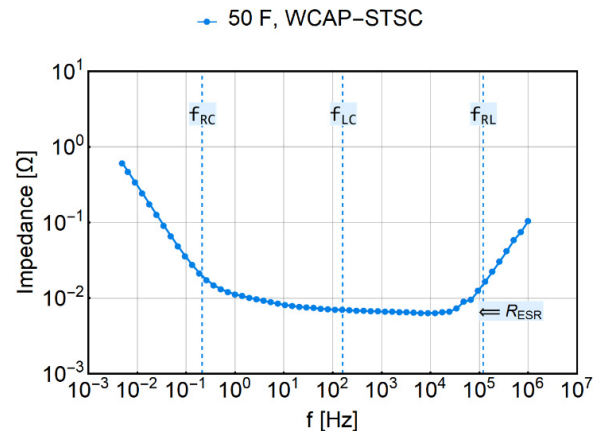

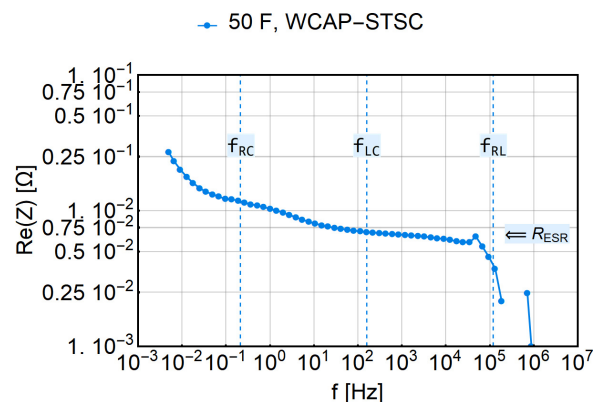Fig. 5. Measured impedance spectrum $|\hat{Z}|$ of 50 F Supercapacitor, WCAP-STSC.

Fig. 6. Measured spectrum of the real part of the impedance ($\text{Re}(\hat{Z}) = R_{ESR}$) of 50 F Supercapacitor, WCAP-STSC.

This frequency dependence is not a measurement artifact, however, attributed to real physical phenomena:

- Distributed network of porous electrodes and
- The ionic charge transport in the electrolyte of the EDLC.[4,6,7,12–14]

A physical interpretation of the spectra is as follows. The slower the SC is charged, the more pores can be infiltrated by charges, which leads to the increase of capacitance. Due to the viscous solvent, the ions require more time to insert the smaller pores, which in turn leads to an increase of R_{ESR} toward low frequencies.

The values of $\mathrm{Re}(\hat{Z}) = R_{\mathrm{ESR}}$ below f_{RC} and above f_{LC} become unreliable, since the spectra become dominated by the capacitive and parasitic inductive behavior.

The shoulder at f_{Leak} is not visible, since it is practically difficult to measure toward such low frequencies. (Also for other capacitor technologies, it is not common practice to measure at such low frequencies. The shoulder at f_{Leak} is usually not depicted in impedance spectra.)

The capacitance spectrum in Fig. 7 shows the typical shoulder situated at the characteristic frequency of the $R_{\mathrm{ESR}} - C$ unit f_{RC}. The height of the shoulder is at about 51 F (0.01 Hz) with a slight increase toward lower frequencies. This increase is especially pronounced in electrolytic capacitors such as Supercaps. It is, as already mentioned above, mainly caused by the charge storing at porous interfaces as well as pseudo-capacitive processes. Mathematically, it can be well described by a set of distributed R-C networks.[3]

The characteristic frequency is, as shown above, governed by the term $R_{\mathrm{ESR}} C_S$. Due to the relatively high capacities, the characteristic frequency shifts to frequencies around or even below 1 Hz. The indicated frequency f_{RC} in Fig. 7 is about 0.21 Hz. The inverse of f_{RC} can be interpreted as lower limit for the constant voltage charging time, which in this case is

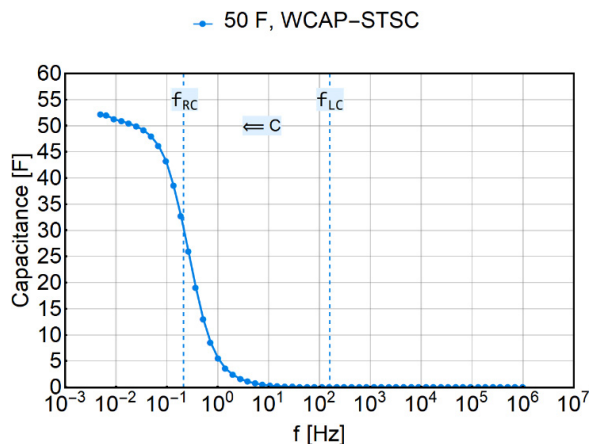$$\frac{1}{f_{\mathrm{RC}}} = \frac{1}{0.21\,\mathrm{Hz}} \approx 5\,\mathrm{s}.$$

The following characteristic values can be extracted from the measured spectra above:

- $C_S(0.01\,\mathrm{Hz}) = 51\,\mathrm{F}$,
- $R_{\mathrm{ESR}}(f_{\mathrm{RC}} = 0.2\,\mathrm{Hz}) = 0.012\,\Omega$,
- $R_{\mathrm{ESR}}(f_{\mathrm{LC}} = 160\,\mathrm{Hz}) = 0.007\,\Omega$.

2.3. *Aluminum electrolytic capacitors, WCAP-AIG8*

The following spectra were measured with the impedance analyzer Alpha-AK, POT/GAL from Novocontrol in a four-terminal Kelvin configuration.

In principle, the charge storing mechanism of the aluminum electrolytic capacitor (E-Cap) is comparable to the one of the SC. The energy is stored by electrolytic charges at a porous interface. However, the E-Cap utilizes a thin porous aluminum oxide layer as a dielectric. The porosity of this layer again leads to large effective surfaces and relatively large capacitance. It is due to the large capacitance that for this type of capacitor f_{RC} is often (not always!) still lower than f_{LC}, as indicated in the measured impedance spectrum of a 270 μF capacitor in Fig. 8. Compared to the SC, f_{LC} has shifted towards higher frequencies. The capacitive contribution is more pronounced and thus appears also further shifted to higher frequencies. The contribution of the parasitic inductance is about the same. Hence, the flat bottom region is much smaller than for the SC.

In general, all features of the spectra in Figs. 9 and 10 appear shifted to higher frequencies. The interpretation of the capacitance spectrum in Fig. 9, with its characteristic shoulder, is similar to the one for the SC.

The equivalent series resistance $\mathrm{Re}(\hat{Z}) = R_{\mathrm{ESR}}$, given in Fig. 10 also shows the increase toward low frequencies. However, below 1 kHz or so, the spectrum shows an increase toward lower frequencies. This increase is, however, probably not due to any real physical effect, it is a measurement artifact. It is a common effect that always happens, if the loss angle is very close to zero. In this region, the equipment is not
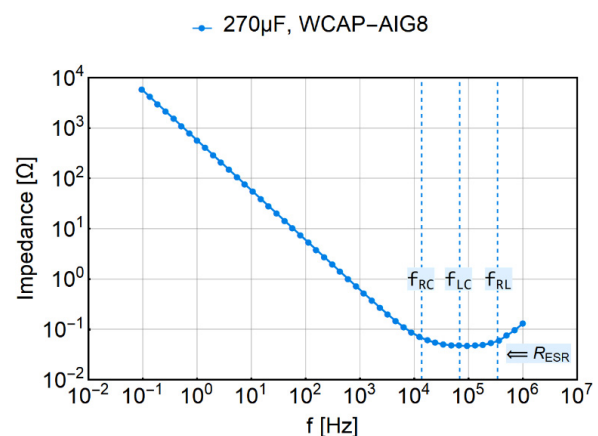

Fig. 7. Measured capacitance spectrum of 50 F Supercapacitor, WCAP-STSC.

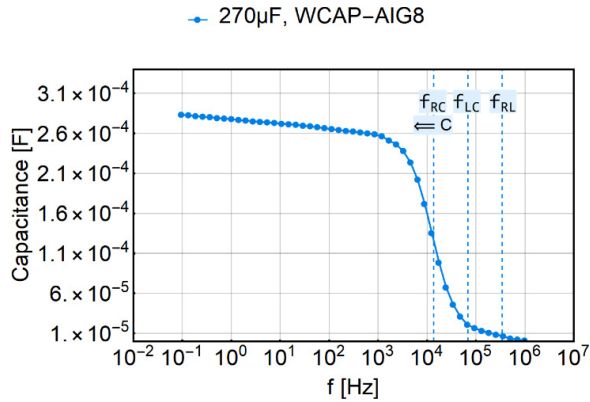Fig. 8. Measured impedance spectrum $|\hat{Z}|$ of 270 μF aluminum electrolytic capacitor.

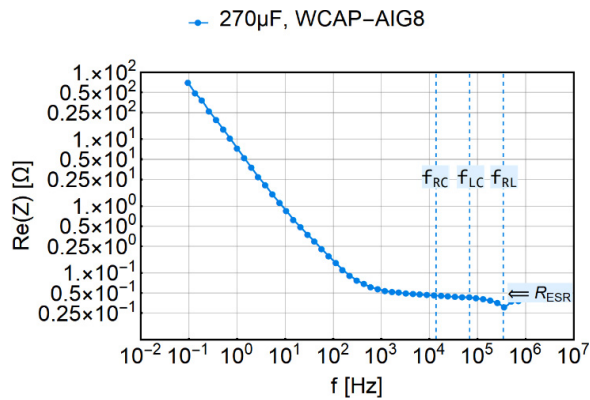Fig. 9. Measured capacitance spectrum of 270 μF aluminum electrolytic capacitor.

Fig. 10. Measured spectrum of the real part of the impedance ($\mathrm{Re}(\hat{Z}) = R_{\mathrm{ESR}}$) of 270 μF aluminum electrolytic capacitor.

able to clearly separate the real and imaginary part from each other, which results in an overestimated output of the real part.

Hence, the correct interpretation of the spectra at low loss angles, which corresponds to low or high frequencies with respect to f_{LC}, is usually difficult, since the loss angle resolution of most LCR meters is not smaller than 0.1 degree or so. However, that also means that generally, the values around or at f_{LC} are most trustworthy.

In the end, a correct interpretation of any impedance spectra is only possible with the experimental details of the measurement.

The following characteristic values can be extracted from the measured spectra above. The dissipation factor DF = $\frac{R_{\mathrm{ESR}}}{X_c} = 2\pi f C_S R_{\mathrm{ESR}}$ is stated to improve the comparability with datasheets and other documentations. The results for frequencies $\ll f_{\mathrm{LC}}$ are given for the sake of completeness. They may contain a large error, as explained in the Appendix and elsewhere.[11,15–17]

- $C_S(120\,\mathrm{Hz}) = 265\,\mu\mathrm{F}$
- $R_{\mathrm{ESR}}(120\,\mathrm{Hz}) = 0.14\,\Omega$

- $R_{\mathrm{ESR}}(f_{\mathrm{LC}} = 68.5\,\mathrm{kHz}) = 0.04\,\Omega$
- $\mathrm{DF}(120\,\mathrm{Hz}) = \frac{R_{\mathrm{ESR}}}{X_c} = 2\pi f C_S R_{\mathrm{ESR}} = 2.8\%$
- $\mathrm{DF}(f_{\mathrm{LC}} = 68.5\,\mathrm{kHz}) = 2\pi f C_S R_{\mathrm{ESR}} = 0.8\%.$

(Capacitive Reactance: $X_c = \frac{1}{2\pi f C_s}$).

2.4. *Film capacitors, WCAP-FTBE*

The spectra below were measured with Agilent E5061B Network Analyzer in a shunt-through configuration.[16]

The measured impedance spectrum of a 470 nF Film capacitor, in Fig. 11, shows in principle the same features as the calculated spectra, given in Fig. 3 (Top). Due to the low capacitance $f_{\mathrm{RC}} > f_{\mathrm{LC}}$, as indicated by the dashed lines, which results in a graph with a sharp minimum at $f_{\mathrm{LC}} = 1.94\,\mathrm{MHz}$. The resistance value at the minimum is roughly the R_{ESR} at f_{LC}, which in this case is about $0.04\,\Omega$.

The measured spectrum of the equivalent series resistance $\mathrm{Re}(\hat{Z}) = R_{\mathrm{ESR}}$, given in Fig. 12, shows a U-like shape with a minimum around f_{LC}. The increase at high and low frequencies is very likely not the actual physically correct ESR behavior of the capacitor, but a measurement artifact from the low capacitance (high impedance) and the parasitic inductance.

The separation of a small real part from a large imaginary part is technically difficult. In the end, the accuracy and the resolution of the measurable loss angle, i.e., phase angle, determine the accuracy of the measured impedance. Accuracy plots for the equipment used (Figs. A.6–A.8) and an error calculation for this measurement are given in the Appendix. In these demanding conditions, analyzers often overestimate $\mathrm{Re}(\hat{Z})$.[11,15,16]

The network analyzer has no separate current and voltage connections, which usually leads to a lower phase accuracy than for four-terminal Kelvin configurations. Hence, it is a common phenomenon that ESR values, if measured in such a configuration, are overestimated. For the sake of prudence, it is best to consider those values as conservative estimates.
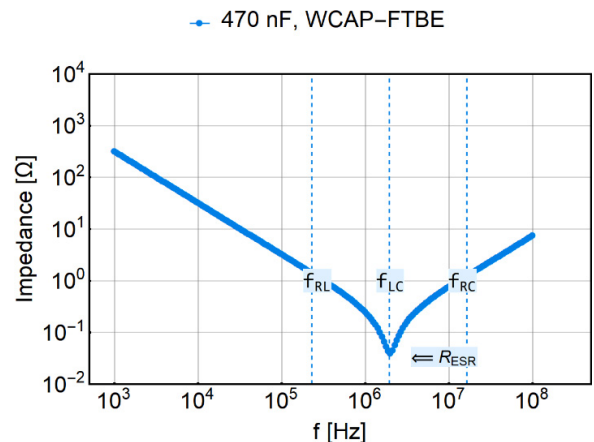

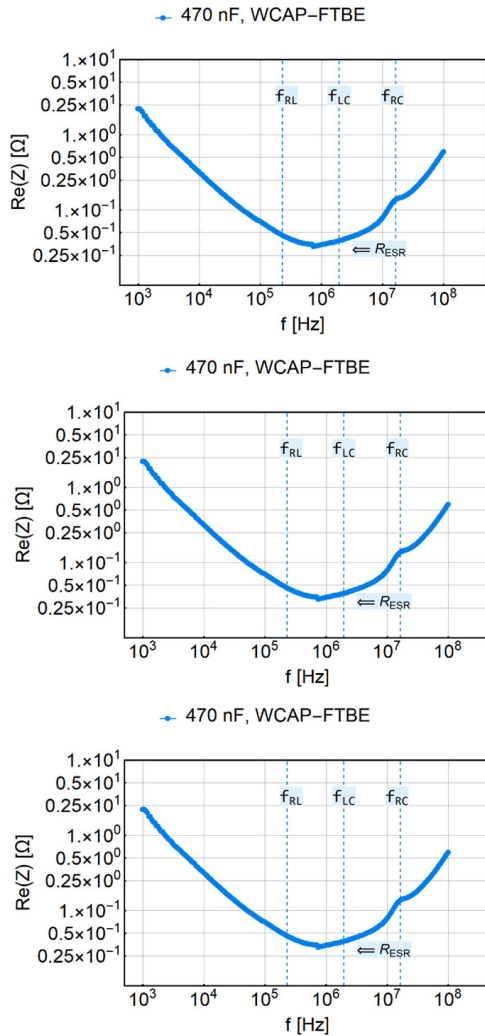Fig. 11. Measured impedance spectrum $|\hat{Z}|$ of 470 nF film capacitor.

Fig. 12. Measured spectrum of the real part of the impedance ($\mathrm{Re}(\hat{Z}) = R_{\mathrm{ESR}}$) of a 470 nF film capacitor. Compare to Fig. 11.

Hence, it is practically difficult to say to what extent the measured $\mathrm{Re}(\hat{Z})$ in Fig. 12 is correct. Certainly, around f_{LC} the results of approximately $0.04\,\Omega$ are most trustworthy and can be considered as conservative estimates. This position is marked by a sharp minimum in Fig. 11.

The measured capacitance spectrum in Fig. 13 shows the overall features of the calculated spectrum, given in Fig. 4. It has a plateau region at low frequencies and a singularity, positioned at f_{LC}. The measured capacitance, as read from the plateau region, is about 495 nF. The measured capacitance with its hyperbolic behavior is physically correct and not some sort of measurement artifact (see Sec. 2).

The parasitic inductance may change as a function of the length of circuit path or temperature. As a consequence, also the position of f_{LC} may change accordingly. It is therefore in practice important to operate the application not in the vicinity of f_{LC}.

The following characteristic values can be extracted from the measured spectra above. The dissipation factor
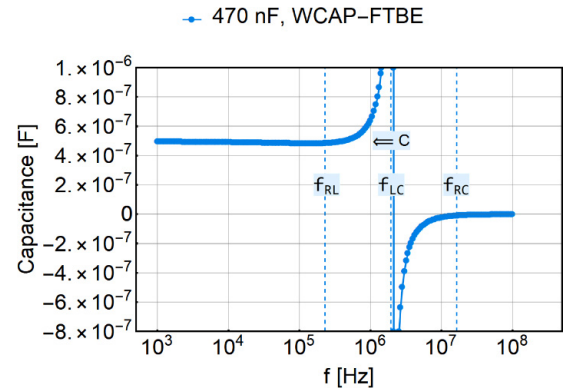

Fig. 13. Measured capacitance spectrum of a 470 nF film capacitor.

$\mathrm{DF} = \frac{R_{\mathrm{ESR}}}{X_c} = 2\pi f C_S R_{\mathrm{ESR}}$ is calculated to improve comparability with datasheets and other documentation. The results for frequencies $\ll f_{\mathrm{LC}}$ are given for the sake of completeness. They may contain a large error as explained in the Appendix and elsewhere.[11,15–17]

- $C_S(1\,\mathrm{kHz}) = 495\,\mathrm{nF}$,
- $R_{\mathrm{ESR}}(1\,\mathrm{kHz}) = 2.2\,\Omega$,
- $R_{\mathrm{ESR}}(f_{\mathrm{LC}} = 1.94\,\mathrm{MHz}) = 0.04\,\Omega$,
- $\mathrm{DF}(1\,\mathrm{kHz}) = 2\pi f C_S R_{\mathrm{ESR}} = 0.68\%$,
- $\mathrm{DF}(f_{\mathrm{LC}} = 1.94\,\mathrm{MHz}) = 2\pi f C_S R_{\mathrm{ESR}} = 24\%$.

2.5. *Multilayer ceramic chip capacitor, WCAP-CSGP*

The following spectra were measured with Agilent E5061B Network Analyzer in a shunt-through configuration.

The impedance spectrum, given in Fig. 14, is qualitatively the same as for the film capacitor in Sec. 2.4. Due to the lower rated capacitance of 22 nF the impedance spectrum is shifted to higher frequencies with $f_{\mathrm{LC}} = 45.8\,\mathrm{MHz}$. As in the previous section $f_{\mathrm{RC}} > f_{\mathrm{LC}}$, which leads to a sharp minimum at f_{LC}.

The ESR, as inferred from the minimum at f_{LC}, is about $0.06\,\Omega$, which for the same reasons as discussed in Sec. 2.4,
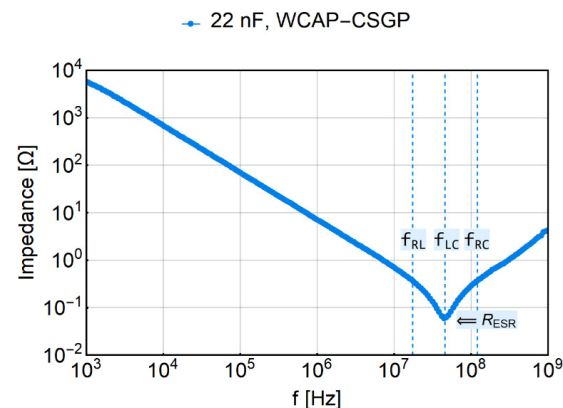

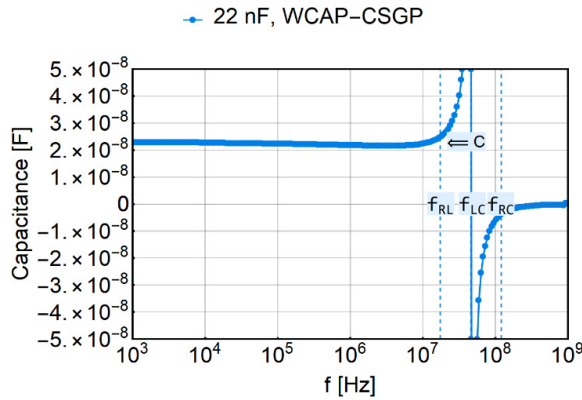Fig. 14. Measured impedance spectrum $|\hat{Z}|$ of 22 nF MLCC.

Fig. 15. Measured capacitance spectrum of 22 nF MLCC.

could be considered as a conservative estimate. The actual ESR might be even lower.

The capacitance spectrum in Fig. 15 shows, as discussed above, the typical resonant behavior. From its constant plateau region, we may read a capacitance of about 23 nF.

Fig. 16 shows the ESR spectrum with a shallow U-like shape. As discussed in the previous section, the increase toward low and high frequencies is probably the result of incorrect separation of real and imaginary part of the impedance by the measurement equipment, i.e., small loss angle δ.

The increase toward lower frequencies could be partially explained by the increase in dielectric loss due to ionic polarization of larger domain structures or charge hopping-induced conductivity. However, the actual value of about $\mathrm{Re}(\hat{Z}) = 3000\,\Omega$ at 1 kHz clearly suggests, that the increase is largely attributed to an insufficient resolution of the loss angle. As mentioned before, it is technically difficult to separate the real part from a relatively large imaginary part, i.e., small loss angle (see Appendix A, Fig. A.7).

The increase toward higher frequencies could be due to the skin effect. The geometrical factor of the electrodes of an MLCC makes a scientifically sound analysis of this effect
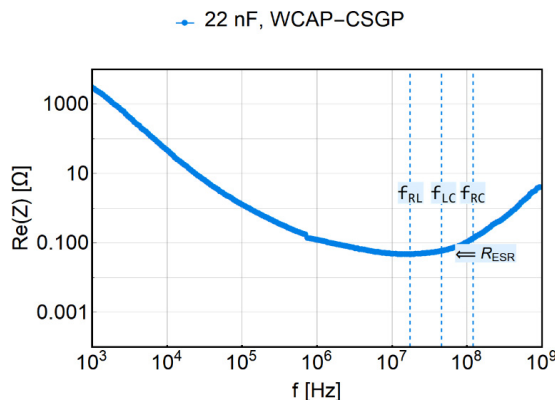

Fig. 16. Measured spectrum of the real part of the impedance ($\mathrm{Re}(\hat{Z}) = R_{\mathrm{ESR}}$) of 22 nF MLCC.

difficult. Usually, studies of skin effect are conducted on cylindrical geometries. Those results cannot be quantitatively used for measurements of MLCCs.[18-20]

Due to the resolution limits of the loss angle, the $\mathrm{Re}(\hat{Z}) = R_{\mathrm{ESR}}$ spectra have often a minimum around f_{LC} and strongly increasing slopes toward low and high frequencies. This measurement effect will superimpose any potential skin effect (see Fig. A.9).[18]

To cut a long story short, ESR spectra of LCR resonators are most trustworthy in the region around f_{LC}. Beyond that, they require, not always but often, further technical knowledge for interpretation.

The following characteristic values can be extracted from the measured spectra above. The dissipation factor $\mathrm{DF} = \frac{R_{\mathrm{ESR}}}{X_c} = 2\pi f C_S R_{\mathrm{ESR}}$ is given to improve comparability with datasheets and other documentations. The results for frequencies $\ll f_{\mathrm{LC}}$ are given for the sake of completeness. They may contain a large error, as explained in the Appendix and elsewhere.[11,15-17]

- $C_S(1\,\mathrm{kHz}) = 23\,\mathrm{nF}$,
- $R_{\mathrm{ESR}}(f_{\mathrm{LC}} = 46\,\mathrm{MHz}) = 0.06\,\Omega$,
- $\mathrm{DF}(f_{\mathrm{LC}} = 46\,\mathrm{MHz}) = 2\pi f C_S R_{\mathrm{ESR}} = 38\%$.

3. Conclusion

The standard model, given in Fig. 1, is a suitable means to interpret the technically important features of all commercially relevant capacitors. In most cases, it is even sufficient to use an even simpler model, which neglects R_{Leak}. It was furthermore demonstrated how the model parameters, such as C_S and R_{ESR}, can be extracted from the measured spectra.

The deviations from that model as well as aspects of the measurement accuracy have been exemplarily discussed on the measured spectra. Especially, the separation of real and imaginary part at small loss angles is defective. In the self-resonant case, the R_{ESR} spectra can only be correctly measured around f_{LC}. Due to this reason, the physical phenomena, such as skin effect, are very likely superimposed by a large error and cannot be studied in the measured R_{ESR} spectra.

Appendix A. Graphs and Figures

Interpretation of $\mathrm{Im}(\hat{C})$ (Fig. A.1) for R-C unit: $\mathrm{Im}(\hat{C})$ describes the dissipation of energy in a capacitive system, associated with the movement of charges. This dielectric relaxation, i.e., absorption band, is caused by the reorientation
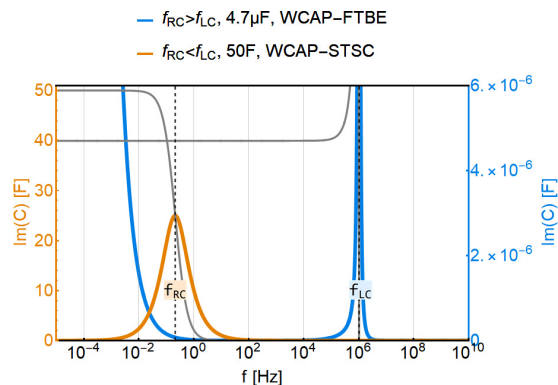
Fig. A.1. Capacitance spectrum $\text{Im}(\hat{C})$ as calculated from the standard model. Corresponds to spectrum $\text{Re}(\hat{C})$ in Fig. 4. Gray lines indicate $\text{Re}(\hat{C})$.
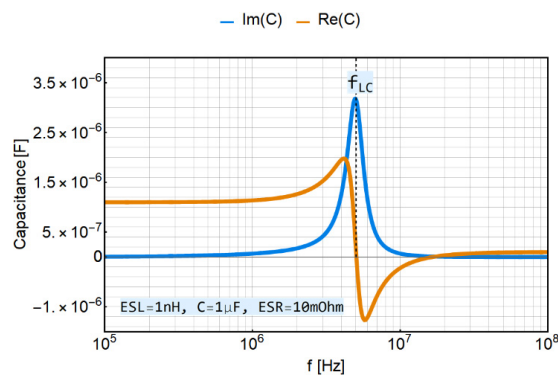

Fig. A.2. Example of calculation for a Lorentz relaxation ($f_{RC} > f_{LC}$), Parameters are such as to see all details.

of permanent molecular dipoles, induced by the applied alternating electric field.

$\text{Im}(\hat{C})$ is mathematically related to the $\text{Re}(\hat{C})$ by the Kramers–Kronig relation. In case of a Debye relaxation, Im
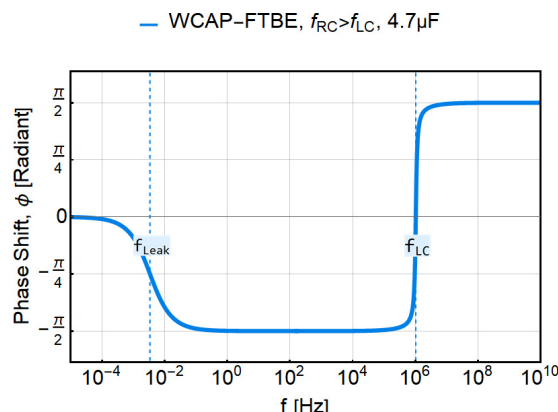

Fig. A.3. Phase shift angle $\phi(f)$ for WCAP-FTBE as calculated from the standard model. Corresponds to impedance spectra in Fig. 3 (top). Polarization contributions at higher frequencies, such as electronic polarizations, are neglected, i.e., $C(f \to \infty) = 0$.
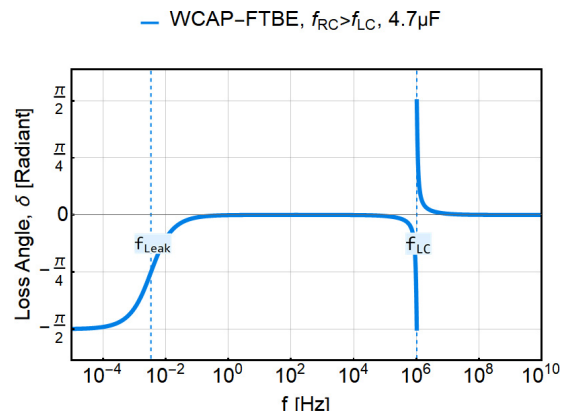

Fig. A.4. Loss angle $\delta(f)$ for WCAP-FTBE as calculated from the standard model. Corresponds to impedance spectra in Fig. 3 (top). Polarization contributions at higher frequencies, such as electronic polarizations, are neglected, i.e., $C(f \to \infty) = 0$.
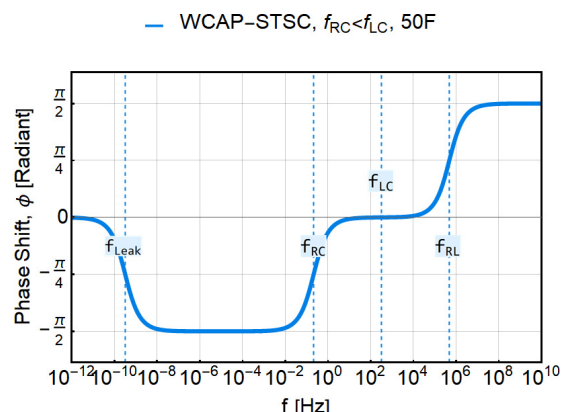

Fig. A.5. Phase shift angle $\phi(f)$ for WCAP-STSC as calculated from the standard model. Corresponds to impedance spectra in Fig. 3 (bottom). Polarization contributions at higher frequencies, such as electronic polarizations, are neglected, i.e., $C(f \to \infty) = 0$.
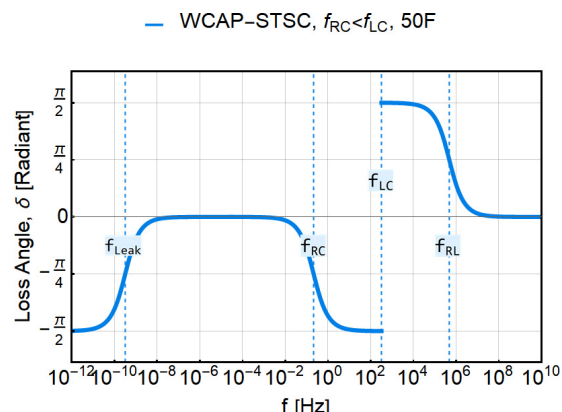

Fig. A.6. Loss angle $\delta(f)$ for WCAP-STSC as calculated from the standard model. Corresponds to impedance spectra in Fig. 3 (bottom). Polarization contributions at higher frequencies, such as electronic polarizations, are neglected, i.e., $C(f \to \infty) = 0$.
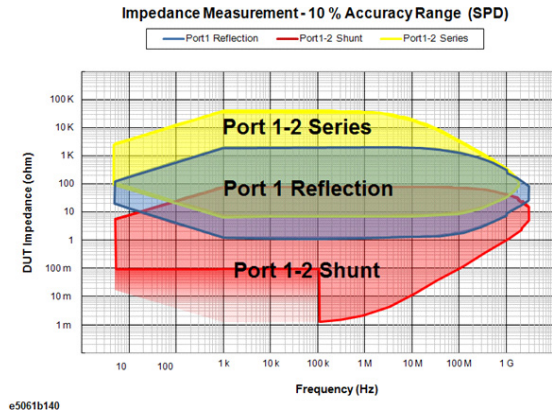
Fig. A.7. Accuracy plot for E5061B ENA Vector Network Analyzer from Keysight. Conditions for 10% measurement accuracy range.[16]
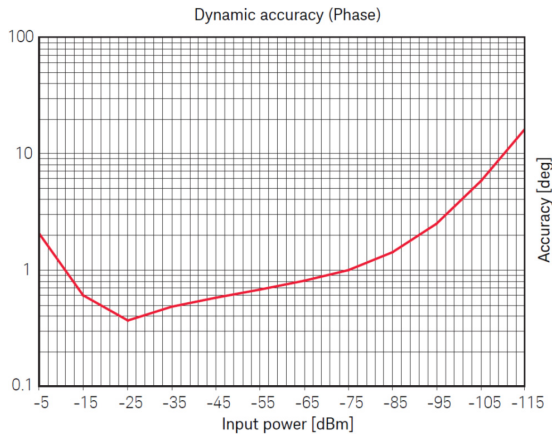

Fig. A.8. Phase accuracy for E5061B ENA Vector Network Analyzer from Keysight.[16,17]

$(\hat{C})$ can be conveniently used to read off f_{RC}. The height of the peak of $\mathrm{Im}(\hat{C})$ at f_{RC} is for the Debye relaxation $C_S/2$.

An example of calculation for a Lorentz oscillation ($f_{\mathrm{RC}} > f_{\mathrm{LC}}$) is given in Fig. A.2. The parameters for the plot are such as to show all details of the curve progression. The graph does not necessarily correspond to a specific capacitor product.

Appendix B. Formulas and Notes

Mathematical description of the equivalent circuit in Sec. 1.1 (temporal frequency: f, angular frequency: $\omega = 2 \cdot \pi \cdot f$)

$$\hat{Z}(\omega) = R_{\mathrm{ESR}} + i \cdot \omega L_{\mathrm{ESL}} + \frac{R_{\mathrm{Leak}}(i\omega C_S)^{-1}}{R_{\mathrm{Leak}} + (i\omega C_S)^{-1}}, \quad \text{(B.1)}$$

$$\hat{Z}(\omega) = \mathrm{Re}(\hat{Z}) + i \cdot \mathrm{Im}(\hat{Z}), \quad \text{(B.2)}$$

$$\mathrm{Re}(\hat{Z}) = \frac{\omega^2 R_{\mathrm{ESR}} R_{\mathrm{Leak}}^2 C_S^2 + R_{\mathrm{ESR}} + R_{\mathrm{Leak}}}{\omega^2 R_{\mathrm{Leak}}^2 C_S^2 + 1}, \quad \text{(B.3)}$$

$$\mathrm{Im}(\hat{Z}) = \frac{\omega(\omega^2 R_{\mathrm{Leak}}^2 L_{\mathrm{ESL}} C_S^2 - R_{\mathrm{Leak}}^2 C_S + L_{\mathrm{ESL}})}{\omega^2 R_{\mathrm{Leak}}^2 C_S^2 + 1}, \quad \text{(B.4)}$$

$$\hat{Z}(\omega) = \frac{\begin{array}{c}(i\omega)^2 R_{\mathrm{Leak}} L_{\mathrm{ESL}} C_S + i\omega(R_{\mathrm{ESR}} R_{\mathrm{Leak}} C_S + L_{\mathrm{ESL}}) \\ + R_{\mathrm{ESR}} + R_{\mathrm{Leak}}\end{array}}{i\omega R_{\mathrm{Leak}} C_S + 1} \quad \text{(B.5)}$$

In electrical engineering, $\mathrm{Re}(\hat{Z})$ and $\mathrm{Im}(\hat{Z})$ are referred to as equivalent series resistance and equivalent series reactance, respectively. The dissipation factor DF is calculated by

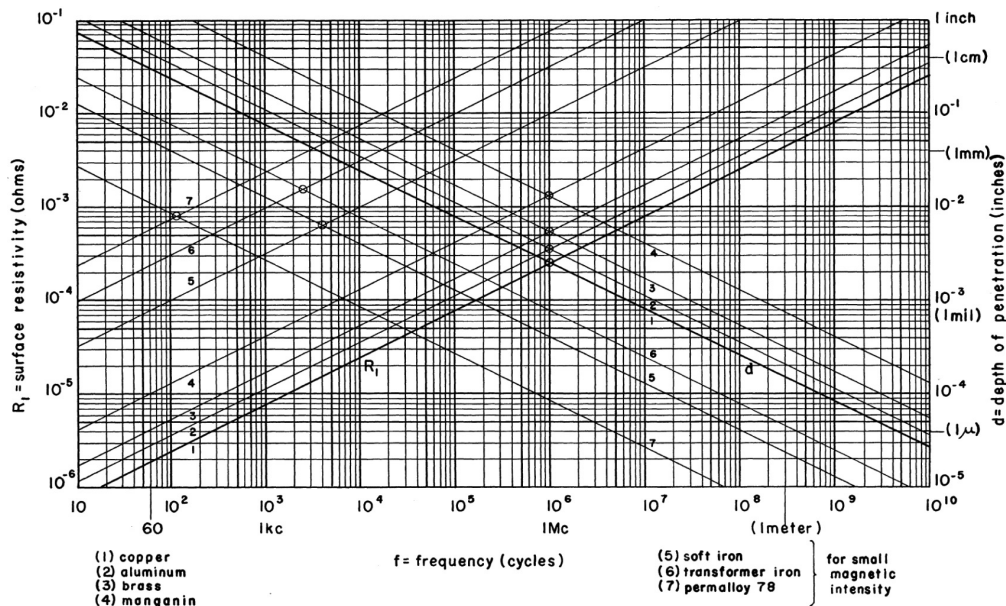$$\mathrm{DF} = \frac{\mathrm{Re}(\hat{Z})}{\mathrm{Im}(\hat{Z})}, \quad \text{(B.6)}$$

Fig. A.9. Surface resistivity and depth of penetration for different materials at room temperature.[18]

$$\text{DF} = \frac{\omega^2 R_{\text{ESR}} R_{\text{Leak}}^2 C_S^2 + R_{\text{ESR}} + R_{\text{Leak}}}{\omega(\omega^2 R_{\text{Leak}}^2 L_{\text{ESL}} C_S^2 - R_{\text{Leak}}^2 C_S + L_{\text{ESL}})}. \qquad \text{(B.7)}$$

With the relation $\hat{Z} = \frac{1}{i\omega C}$, capacitance is calculated under the simplification that

$$R_{\text{Leak}} \to \infty \hat{C}(\omega) = \frac{L_{\text{ESL}}}{k} + \frac{1}{k\omega^2 C_S} - i\frac{R_{\text{ESR}}}{k\omega}, \qquad \text{(B.8)}$$

with $k = (\omega L_{\text{ESL}} - \frac{1}{\omega C_S})^2 + R_{\text{ESR}}^2$.

If additionally $L_{\text{ESL}} \to 0$, it follows:

$$\hat{C}(\omega) = \frac{C_S}{1 + (\omega R_{\text{ESR}} C_S)^2} - i \cdot \frac{\omega C_S^2 R_{\text{ESR}}}{1 + (\omega R_{\text{ESR}} C_S)^2}. \qquad \text{(B.9)}$$

The characteristic frequency of the $R_{\text{ESR}} - C$ unit: Solution of equation $\text{Im}[\hat{C}(f_{\text{RC}})] = C_s \frac{1}{2}$ is as follows:

$$f_{\text{RC}} = \frac{1}{2 \cdot \pi \cdot R_{\text{ESR}} \cdot C_S}. \qquad \text{(B.10)}$$

Characteristic frequency of the $L - C$ unit:
Solution of $\text{Im}(\hat{Z}(\omega_{\text{LC}})) = 0$ yields

$$\omega_{\text{LC}} = 2\pi f_{\text{LC}} = \frac{1}{\sqrt{L_{\text{ESL}} \cdot C_S}}. \qquad \text{(B.11)}$$

Characteristic frequency of the $R_{\text{Leak}} - C$ unit ($R_{\text{Leak}} \to \infty$):

A pole of Eq. (B.5) is a zero of $i\omega R_{\text{Leak}} C_S + 1$. The solution of $i(2\pi f_{\text{Leak}})R_{\text{Leak}} C_S + 1 = 0$ yields

$$f_{\text{Leak}} = \frac{i}{2 \cdot \pi \cdot R_{\text{Leak}} \cdot C_S}. \qquad \text{(B.12)}$$

For the sake of simplicity, we keep the formula sign for the absolute value:

$$f_{\text{Leak}} = \frac{1}{2 \cdot \pi \cdot R_{\text{Leak}} \cdot C_S}. \qquad \text{(B.13)}$$

Characteristic frequency of the $R_{\text{ESR}} - L$ unit ($R_{\text{Leak}} \to \infty$):

Solution of $0 = R_{\text{ESR}} - 2\pi f_{\text{RL}} L_{\text{ESL}}$ for f_{RL} yields

$$f_{\text{RL}} = \frac{R_{\text{ESR}}}{2 \cdot \pi \cdot L_{\text{ESL}}}.$$

Effect of limited loss angle resolution:

Table B.1. Values for exemplary error calculation.

Parameter	Value	Value	Value
f_e in kHz	450	10	1
$\text{Im}(\hat{Z})$ in Ω, $C_S = 4.7$ nF	0.75	33.86	338.63
$\text{Re}(\hat{Z})$ at f_e in Ω	0.039	0.31	2.23
δ_Δ in° (Fig. A.8)	0.30	0.30	0.30
$\tan\delta$	0.052	0.009	0.007
δ in°	2.967	0.525	0.377
Δ in %	10.1	57.2	79.5

Since the analyzer cannot measure loss angles below its resolution limit, DF will assume its minimum and remain constant for high and low frequencies (with respect to f_{LC}). Consequently, in those high- and low-frequency regimes, the ESR will become proportional to the reactance, with DF as proportionality factor. Therefore, measured ESR spectra will often show a bathtub-like shape, where the position of the minimum of the ESR spectra coincides with the minimum of the impedance spectra.

To access the accuracy of the measured ESR, it is always necessary to consider the phase angle resolution. If the measured loss angle or DF is at the resolution limit of the analyzer, it is difficult to retrieve the correct ESR spectra.

Example of calculation of loss angle measurement error with loss angle resolution limit δ_Δ:

The relative error associated with the $\tan\delta$ is calculated by

$$\Delta = \frac{\tan(\delta + \delta_\Delta) - \tan\delta}{\tan\delta} \cdot 100\%. \qquad \text{(B.14)}$$

The results for the measured frequencies f_e in Table are calculated on the basis of spectra, given in Fig. 12. They exemplify the error Δ associated with the measurement of the above film capacitors (WCAP-FTBE).

References

[1] E. Barsoukov and J. R. Macdonald (eds.), *Impedance Spectroscopy: Theory, Experiment, and Applications*, 3rd edn. (John Wiley & Sons, Hoboken, NJ, 2018).

[2] L. Moura and I. Darwazeh, *Introduction to Linear Circuit Analysis and Modelling: From DC to RF* (Elsevier, Oxford, 2005).

[3] B. E. Conway, *Electrochemical Supercapacitors — Scientific Fundamentals and Technological Applications* (Kluwer Academic Publishers, Springer, Boston, 1999).

[4] M. Schönleber and E. Ivers-Tiffée, Approximability of impedance spectra by RC elements and implications for impedance analysis, *Electrochem. Commun.* **58**, 15 (2015).

[5] E. Ivers-Tiffée and Aweber, Evaluation of electrochemical impedance spectra by the distribution of relaxation times, *J. Ceram. Soc. Jpn.* **125**, 193 (2017).

[6] V. Srinivasan and J. W. Weidner, Mathematical modeling of electrochemical capacitors, *J. Electrochem. Soc.* **146**, 1650 (1999).

[7] M. R. Hasyim, D. Ma and R. Rajagopalan and C. Randall, *Electrochem. Soc.* **164**, A2899 (2017).

[8] J.-S. Lee *et al.*, Impedance spectroscopy models for X5R multilayer ceramic capacitors, *J. Korean Ceram. Soc.* **49**, 475 (2012).

[9] A. F. J. Levi, *Essential Classical Mechanics for Device Physics* (Morgan & Claypool Publishers, San Rafael, CA, 2016).

[10] R. M. Hill and L. A. Dissado, Debye and non-Debye relaxation, *J. Phys. C. Solid State Phys.* **18**, 3829 (1985).

[11] D. Edwards, J.-H. Hwang, S. J. Ford and T. O. Mason, Experimental limitations in impedance spectroscopy: Part V. Apparatus contributions and corrections, *Solid State Ion.* **99**, 85 (1997).

[12] R. Kötz *et al.*, Temperature behavior and impedance fundamentals of supercapacitors, *J. Power Sources* **154**, 550 (2006).

[13]B.-A. Mei *et al.*, Physical interpretations of nyquist plots for EDLC electrodes and devices, *J. Phys. Chem. C* **122**, 194 (2018).

[14]M. Itagaki, Electrochemical impedance and complex capacitance to interpret electrochemical capacitor, *Electrochemistry* **75**(8), 649 (2007).

[15]T. Stolzke *et al.*, Comprehensive accuracy examination of electrical power loss measurements of inductive components for frequencies up to 1 MHz, *J. Magn. Magn. Mater.* **497**, 166022 (2020).

[16]Online Manual, E5061B Network Analyzer, Keysight, http://ena. support.keysight.com/e5061b/manuals/webhelp/eng/?nid=-32496.1150148.00&cc=CA&lc=eng&id=1790874.

[17]Datasheet, E5061B Network Analyzer, Keysight, http://ena. support.keysight.com/e5061b/manuals/webhelp/eng/product_ information/specifications.htm.

[18]H. A. Wheeler, Formulas for the skin effect, *Proc. IRE* **30**, 412 (1942).

[19]A. E. Kennelly, F. A. Laws and P. H. Pierce, Experimental researches on skin effect in conductors, *Trans. Am. Inst. Electr. Eng.* **34**, 1953 (1915).

[20]G. Schröder, J. Kaumanns and R. Plath, Advanced measurement of AC resistance on skin-effect reduced large conductor power cables, *8th Int. Conf. Insulated Power Cables*, Versailles, France (2011).